(Preprint) AAS 12-034

ADDRESSING THE INFLUENCE OF SPACE WEATHER ON AIRLINE NAVIGATION

Lawrence Sparks*

The advent of satellite-based augmentation systems has made it possible to navigate aircraft safely using radio signals emitted by global navigation satellite systems (GNSS) such as the Global Positioning System. As a signal propagates through the earth's ionosphere, it suffers delay that is proportional to the total electron content encountered along the raypath. Since the magnitude of this total electron content is strongly influenced by space weather, the safety and reliability of GNSS for airline navigation requires continual monitoring of the state of the ionosphere and calibration of ionospheric delay. This paper examines the impact of space weather on GNSS-based navigation and provides an overview of how the Wide Area Augmentation System protects its users from positioning error due to ionospheric disturbances.

INTRODUCTION

Signals emitted by global navigation satellite systems (GNSS) such as the *Global Positioning System* (GPS) are now used routinely throughout the world as a means of determining position. To enable the use of such signals for airline navigation, satellite-based augmentation systems have been developed to enhance the accuracy, availability, continuity, and integrity of user position estimates based upon GNSS signals. In the absence of such augmentation, position estimates are not sufficiently trustworthy to serve as a safe means of guiding aircraft.

In North America, the *Wide Area Augmentation System* (WAAS), an augmentation of the Global Positioning System, measures the delay of signals that propagate from GPS satellites to multiple, dual frequency receivers distributed in a network of thirty-eight reference stations (see Figure 1). WAAS first became available for airline navigation after its commissioning on 10 July 2003. Subsequently the MTSAT Satellite-Based Augmentation System (MSAS) in Japan and the European Geostationary Navigation Overlay Service (EGNOS) in Europe have been commissioned. Other systems worldwide are under development.

The propagation of a GNSS signal through the ionosphere is delayed due the presence of charged particles along the signal raypath. Currently, the ionosphere serves as the largest source of error for aviational users of GPS. To permit a user to correct a position estimate for error due to ionospheric delay, WAAS derives estimates of vertical delay from GPS measurements and broadcasts a vertical delay estimate at each ionospheric grid point (IGP) on a grid specified at regularly spaced intervals of latitude and longitude (see Figure 2). The vertical delay at an IGP is designated the Ionospheric Grid Delay (IGD) at that IGP. Furthermore, WAAS calculates and broadcasts a safety-critical integrity bound at each IGP called the Grid Ionospheric Vertical Error (GIVE). Here *integrity* refers to the reliability and trustworthiness of the broadcast navigation

* Jet Propulsion Laboratory / California Institute of Technology, 4800 Oak Grove Drive, Pasadena, CA 91109.

message and to the WAAS's ability to provide timely warnings to users when the system is not safe to use due to signal corruption or some other system error or failure. Broadcast GIVEs allow the user to bound the actual error of the IGDs with a high degree of certainty. To derive the GIVE, the formal estimation error is inflated to protect the user from the influence of well-sampled ionospheric irregularities and, in addition, it is augmented to protect the user from the consequences of undersampling.

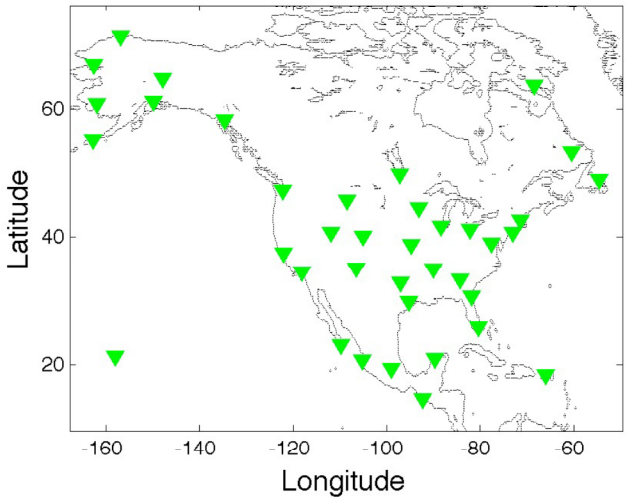

Figure 1. WAAS receiver sites across North America.

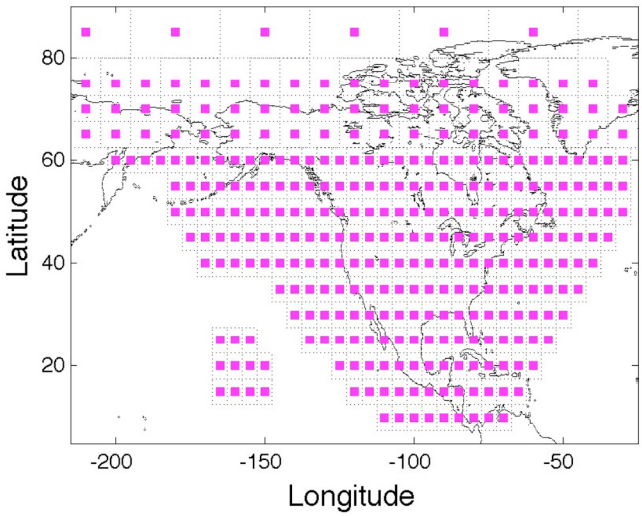

Figure 2. WAAS ionospheric grid points at which IGDs and GIVEs are broadcast.

Space weather exerts enormous influence over the state of the ionosphere. For example, the presence of a severe ionospheric storm can result in large increases in the magnitude of the delay experienced by a GNSS signal propagating through the ionosphere. Of particular concern are highly localized irregularities that interfere with the propagation of signals detected by a user receiver but that are poorly sampled by the measurements of receivers in the system network. The

most challenging conditions have been found to arise following *extreme storms*, *i.e.*, large-scale disturbances that occur only rarely over the course of a solar cycle. Thus, the influence of space weather represents a potential threat to the safety of and reliability of airline navigation based upon GNSS signals. Satellite-based augmentation systems must monitor the state of the ionosphere continuously and provide accurate calibration of ionospheric delays whenever the level of ionospheric disturbance does not exceed a critical threshold that renders the system locally unavailable.

This paper examines the impact of space weather on GNSS-based navigation and provides an overview of how WAAS monitors the state of the ionosphere and protects the user from positioning error due to ionospheric disturbances. The paper is subsequently divided into five sections. The first section reviews how the influence of the ionosphere on radio signals is modeled in WAAS. The second section considers how WAAS estimates the vertical delay values and integrity bounds that are broadcast. The third section discusses how WAAS mitigates three distinct ionospheric threats that arise as a consequence of space weather: well-sampled irregularities, undersampled irregularities, and highly localized irregularities arising under extreme storm conditions. The fourth section describes how WAAS ranks storms according to their magnitude as represented by a scalar metric. The final section presents a summary of the topics discussed.

MODELING THE INFLUENCE OF THE IONOSPHERE ON GPS

The existence of the ionosphere is largely due to photoionization of atmospheric molecules during daylight hours. The delay that a GNSS signal experiences as it passes through the ionosphere is proportional to the number of free electrons along the signal's raypath. The column density of electrons encountered by the signal is called the *total electron content* of the raypath. The slant total electron content (STEC) between a satellite and a receiver may be written as a path integral of electron density along the line-of-sight as follows:

$$\begin{aligned} STEC_{rs} &= \int_{\ell_r}^{\ell_s} d\ell\, n_e\left(\mathbf{x}_{rs}(\ell)\right) \\ &= \int_{h_r}^{h_s} dh\, F(\alpha,h)\, n_e\left(\mathbf{x}_{rs}(h)\right) \end{aligned} \tag{1}$$

where the subscripts r and s identify, respectively, the receiver and satellite associated with the signal, n_e is the ionospheric electron density, and $\mathbf{x}_{rs}(\ell)$ identifies points along the raypath as parameterized by the path length ℓ; the second expression redefines the integral in local Cartesian coordinates as one over altitude h, with

$$F(\alpha,h) \equiv \left[1-\left(\frac{R_e\cos(\alpha)}{R_e+h}\right)^2\right]^{-1/2} \tag{2}$$

where R_e is the earth radius, α is the elevation angle of the satellite as viewed from the receiver, and $\mathbf{x}_{rs}$ is now treated as a function of the altitude h.

To estimate IGDs and evaluate GIVEs, WAAS treats the ionosphere as consisting of charged particles restricted to an infinitesimally thin shell at a representative ionospheric altitude $h = h_{iono}$ (see Figure 3). In practice h_{iono} is chosen to be 350 km, a typical altitude at which the atmospheric electron density attains its maximum. This crude model serves two purposes: (1) it permits us to associate with each measurement an *ionospheric pierce point* (IPP) and (2) it facilitates the

conversion of each slant delay measurement to an estimate of the vertical delay at the IPP. The IPP for a given measurement is the location where the satellite-to-receiver raypath intersects the thin shell. The expression used to convert slant delay to vertical delay, $F(\alpha, h_{iono})$, is designated the *obliquity factor* of the raypath.

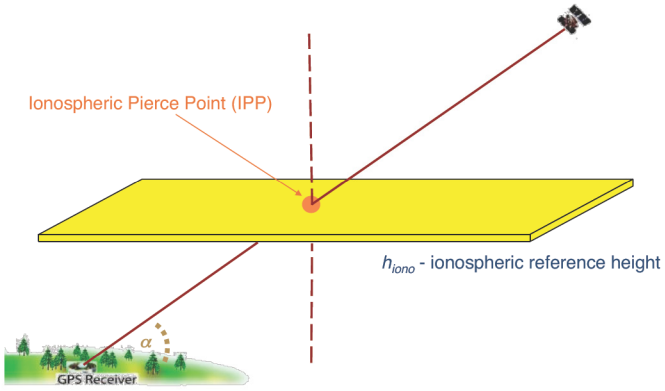

Figure 3. Thin shell model of the ionosphere.

Near an IGP, the vertical ionospheric delay I_{true} at an IPP is modeled as

$$I_{true}(\Delta\mathbf{x}) = a_0 + a_{east}\,\Delta\mathbf{x}^T \cdot \hat{e}_{east} + a_{north}\,\Delta\mathbf{x}^T \cdot \hat{e}_{north} + r(\Delta\mathbf{x}), \tag{3}$$

where $\Delta\mathbf{x} \equiv \mathbf{x} - \mathbf{x}_{IGP}$ is the Euclidean vector describing the distance separating the IPP from the IGP in ECEF Cartesian coordinates, the coefficients a_0, a_{east}, and a_{north} specify the planar trend of the vertical delay, and $r(\Delta\mathbf{x})$ is a scalar field that represents small irregularities that are superimposed on the planar trend. The scalar field provides a means of characterizing the correlation between neighboring measurements. The vertical ionospheric delay measured at $\mathbf{x}$ can then be expressed as

$$I_{meas}(\Delta\mathbf{x}) = I_{true}(\Delta\mathbf{x}) + \varepsilon \tag{4}$$

where ε represents the measurement error. The measurement noise is specific to each receiver-satellite pair and does not depend upon the state of the ionosphere.

This model of vertical delay is valid over spatial scales where the variation of the delay is approximately linear. For larger scales, the magnitude of the scalar field $r(\Delta\mathbf{x})$ will no longer be small.

THE ESTIMATION OF IONOSPHERIC DELAY AND INTEGRITY BOUNDS

WAAS estimates vertical delay (IGDs) at uniformly spaced intervals in time. In a given epoch WAAS first identifies the IPP associated with each measurement and then converts slant delay to vertical delay at that IPP using the appropriate obliquity factor. To estimate the vertical delay at a given IGP, it selects measurements whose IPPs reside in the region near the IGP. The fit domain of the ionospheric shell is the area within a circle centered upon the IGP, whose radius is R_{fit} as measured by the Euclidean (straight-line) separation between the location of the IGP and the points on the circle (see Figure 4). Estimation of the vertical delay at the IGP was initially

achieved by a planar fit of the selected slant measurements, converted to vertical delay. After a recent upgrade of WAAS, however, estimation is now performed by an established, geo-statistical technique known as *kriging*.[1] By this means vertical delay estimates, distributed unevenly in space over the thin shell are transformed into a set of vertical delay estimates distributed at regular spatial intervals on the WAAS ionospheric grid.

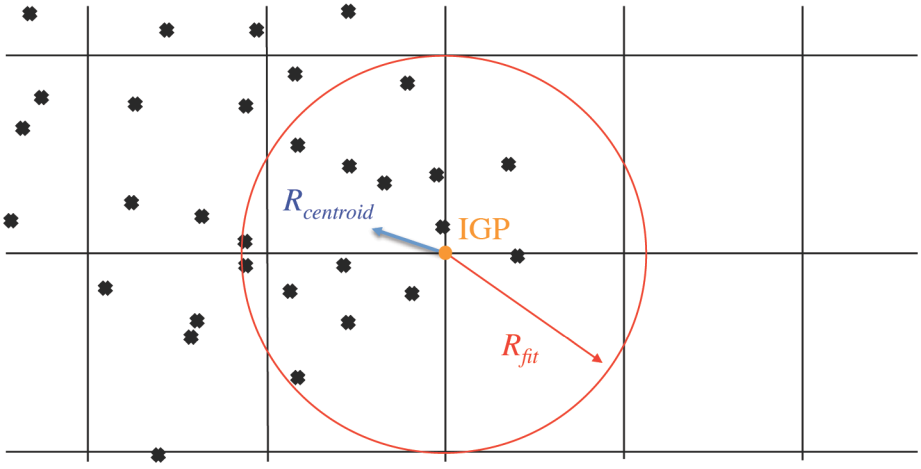

Figure 4. Ionospheric pierce points associated with measurements selected for vertical delay estimation at an ionospheric grid point. Also indicated for the fit IPP distribution are the fit radius R_{fit} and the centroid radius $R_{centroid}$.

To determine the ionospheric slant delay associated with a GPS signal detected by a user's receiver, the WAAS user must first locate the IPP associated with the signal and then approximate the vertical delay at this IPP using bilinear interpolation of the IGDs at the nearest IGPs surrounding the IPP. The interpolated vertical delay estimate is then converted to an estimate of the slant delay from the satellite to the user, using the obliquity factor associated with this signal.

HOW WAAS HANDLES IONOSPHERIC THREATS

To ensure airline navigation safety, the GIVE broadcasted at each IGP must bound the actual IGD estimation error to a very high degree of confidence. Under quiet ionospheric conditions at mid-latitudes, the magnitude of this error is surprisingly small given the crude assumptions about the ionosphere that the model invokes. At low latitudes, however, or at mid-latitudes under disturbed conditions, the error can increase significantly due to the presence of enhanced ionization, complex ionospheric structure, or large electron density gradients.

When the ionosphere becomes sufficiently disturbed, the GIVE evaluated at a given IGP cannot be trusted to bound the vertical delay estimation error. Since it is imperative to know when such a situation exists, WAAS employs an *irregularity detector* to monitor the level of disturbance at each IGP. When disturbances are sufficiently localized, however, the measurements upon which the irregularity detector is based may not sample the region of disturbance adequately, *i.e.*, the irregularity detector may fail to reflect accurately the local level of disturbance. A particularly egregious example of the threat posed by undersampling results from the presence of dense, highly localized disturbances that linger following the occurrence of

an extreme storm. Such events have motivated the implementation of an extreme storm detector in WAAS.

In summary, three distinct types of ionospheric disturbances threaten the accuracy and reliability of the broadcast vertical delay estimates: (1) well-sampled disturbances, (2) undersampled disturbances, and (3) highly localized disturbances that arise under extreme storm conditions. The following subsections will address the manner in which WAAS mitigates the threat posed by each type of disturbance.

The Threat Due To Well-Sampled Ionospheric Irregularities

Associated with each estimate of vertical delay at an IGP is the classical χ^2 goodness-of-fit statistic that describes how well the statistical model fits a given set of measurements. In practice this statistic has been found to be the best indicator of the local level of ionospheric disturbance.[2] Consequently it serves as the basis for the WAAS *irregularity metric*, χ^2_{irreg}. The magnitude of this metric at an IGP is used to indicate whether the IGD at this IGP may be safely accessed by a WAAS user when determining his or her position.

Distributions of this metric reflect the level of ionospheric disturbance across North America over the time duration that the statistics are tabulated. As examples, we consider data from two days exhibiting radically different ionospheric conditions: a quiet day (9 November 2005) and a day on which an extreme storm occurred (30 October 2003). The level of ionospheric disturbance is correlated with the level of geomagnetic disturbance as indicated by two geomagnetic indices, the disturbance storm time index (D_{ST}) and the planetary K-index (K_p). For 9 November 2005, and 30 October 2003, the D_{st} index dropped to -10 and -383 nT, respectively, while the K_p index attained maxima of 2+ and 9, respectively.

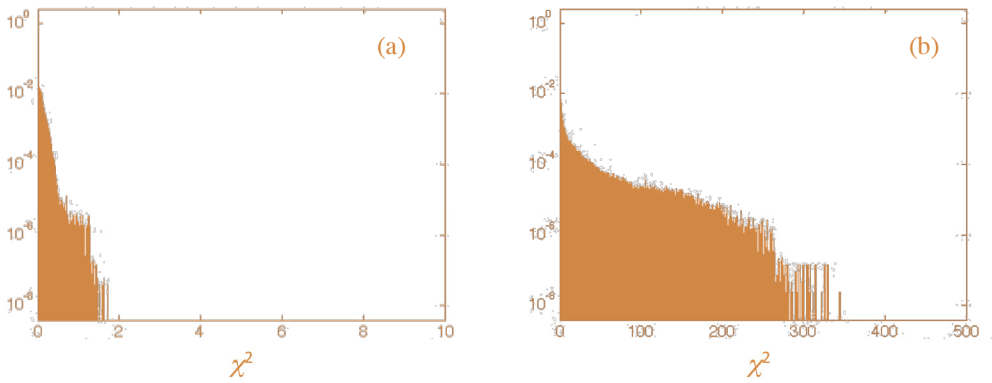

Figure 5. The distribution of the local irregularity metric under (a) quiet ionospheric conditions (9 November 2005) and (b) highly disturbed conditions (30 October 2003).

Figure 5 displays the distribution of the irregularity metric for the two days in question. The vertical scale on each plot has been normalized so that the area under the distribution curve is unity. Note that the maximum value on the horizontal axis has increased by a factor of 50 in the second figure. For the day of quiet conditions, the maximum value, mean value, and standard deviation of the irregularity metric are, respectively, 1.71, 0.075, and 0.076. The same values for the storm day are, respectively, 344.6, 4.9, and 18. Clearly the magnitude of the irregularity metric reflects the local level of ionospheric disturbance.

The broadcast GIVE is dependent upon the formal error variance of the vertical delay estimate at the IGP.[3] Even under nominal ionospheric conditions, however, there is a finite statistical probability that the formal delay error significantly underestimates the true error. Accordingly, the calculation of the GIVE at an IGP uses an inflated version of the formal error variance. The amount of the inflation is proportional to the value of the irregularity metric - the larger the level of ionospheric disturbance, the greater the inflation.

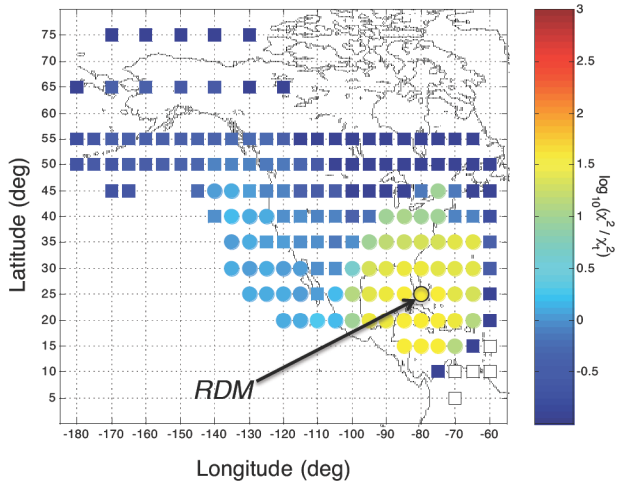

Figure 6. The value of the local irregularity metric at each IGP at 4:43 UTC on the morning of 31 October 2003. The maximum of these values is the value of the regional disturbance metric for North America.

The irregularity detector mitigates the ionospheric threat posed to WAAS by well-sampled disturbances. As an example, Figure 6 shows the value of the irregularity metric at each IGP in the WAAS grid under extremely disturbed conditions that occurred during the Halloween storm of 2003. As the level of local ionospheric disturbance grows, the magnitude of the GIVE increases until the magnitude of the irregularity metric exceeds a critical threshold. At this point, the IGD at the IGP in question is declared not available for positioning. In Figure 6 square symbols indicate IGPs where the irregularity metric lies below the critical threshold; circular disks indicate regions where the irregularity detector has tripped and the IGDs are not available for positioning. In this fashion WAAS warns users where the ionosphere is too disturbed for the user to trust position estimates based upon GNSS measurements.

The Threat Due To Undersampled Ionospheric Irregularities

The contribution of the inflated formal error variance to the GIVE protects the user only from delay error due to ionospheric irregularities that are well sampled by WAAS. Each GIVE, however, must also provide protection from delay error resulting from poor IPP coverage. A disturbance that is not detected by WAAS can nonetheless increase the delay experienced by a signal propagating through it toward a user, and consequently the user's computed position integrity bound will underestimate significantly the true error in the user's position estimate. Thus, in addition to inflating GIVEs to account for the statistical uncertainty of the formal error variance, WAAS augments GIVEs by an additional term designed to shield the user from the threat to delay accuracy constituted by any undersampled irregularities present. The amount of this augmentation is specified by the *undersampled ionospheric irregularity threat model*.[4, 5, 6]

The GIVE at an IGP may be expressed as

$$GIVE = k\sqrt{\sigma_{IGP}^2 + \sigma_{undersampled}^2} \tag{5}$$

where σ_{IGP}^2 is the inflated formal error variance and $\sigma_{undersampled}^2$ is the augmentation provided by the ionospheric threat model (k is a constant). The threat model is designed to handle a worst-case scenario where ionospheric disturbances are almost, but not quite, severe enough to trip the local irregularity detector.

The ionospheric threat model is constructed by requiring that the actual delay estimation error be bounded at any IGP where the irregularity detector has not tripped, as follows:

$$\left|\bar{I}_\kappa - \tilde{I}_\kappa\right|^2 < K_{undersampled}^2 \; \tilde{\sigma}_\kappa^2 \tag{6}$$

where $\bar{I}_\kappa$ is the measured vertical delay at the κ^{th} IPP, $\tilde{I}_\kappa$ is the corresponding estimated value, $\tilde{\sigma}_\kappa^2$ is the inflated variance of the delay estimate, and $K_{undersampled}$ specifies an upper bound on the square of the residual in terms of the inflated formal error. This inequality is always satisfied under quiet ionospheric conditions. Under disturbed conditions, however, it may fail. In this case, $\bar{\sigma}_{undersampled,\kappa}^2$ can be defined by requiring

$$\left|\bar{I}_\kappa - \tilde{I}_\kappa\right|^2 = K_{undersampled}^2 \left[\tilde{\sigma}_\kappa^2 + \bar{\sigma}_{undersampled,\kappa}^2\right] \tag{7}$$

The ionospheric threat model strives to identify the maximum values of $\bar{\sigma}_{undersampled,\kappa}^2$ that can ever be observed as a function of two metrics that characterize the IPP coverage in the vicinity of the IGP.

The first of these metrics, the fit radius R_{fit}, is considered as a scalar metric that characterizes the spatial density of IPPs within the fit domain: the larger the magnitude of R_{fit}, the lower the density and, hence, the higher the probability that an ionospheric irregularity within the fit domain is undersampled. A second scalar that characterizes the spatial distribution of IPPs within the fit domain is the centroid radius $R_{centroid}$ (see Figure 4). When tabulating the threat model, the ratio $R_{centroid}$ / R_{fit} (the *relative centroid metric* or *RCM*), rather than $R_{centroid}$ alone, is used to describe the uniformity of the distribution of IPPs within the fit domain. The larger the magnitude of the *RCM*, the more highly skewed are the IPPs to one side of the IGP and the greater the likelihood that an ionospheric irregularity within the fit domain is undersampled.

The threat model is generated by examining historical data sets consisting of observations recorded under storm conditions. Values of $\bar{\sigma}_{undersampled,\kappa}^2$ are tabulated for IGPs where the irregularity detector has not tripped. At any such IGP, $\bar{\sigma}_{undersampled,\kappa}^2$ is tabulated only for IPPs that lie within the *threat domain* of the IGP. (The dotted lines in Figure 2 show the threat domain associated with each IGP.) The tabulation of the raw data for the undersampled threat model is performed using the following equation:

$$\sigma_{undersampled}^{raw}\left(R_{fit}, RCM\right) = \max_{\text{over } \kappa, T}\left(\sigma_{undersampled,\kappa}\right), \tag{8}$$

and the maximization is performed over measurements κ and over the time interval T following each fit epoch. Figure 7 shows the values of $\sigma_{undersampled}^{raw}$, tabulated using kriging estimation, after processing twenty-one days of data from the largest storms of the last solar cycle. To ensure that

$\sigma_{undersampled}$ increases monotonically with respect to each IPP distribution metric, the actual threat model used by WAAS is defined as the two-dimensional overbound of the raw data. The overbound of the raw data in Figure 7 is displayed in Figure 8.

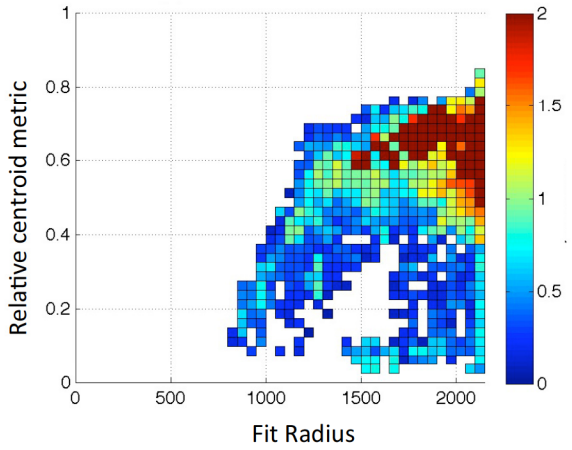

Figure 7. Raw data for the undersampled ionospheric threat model.

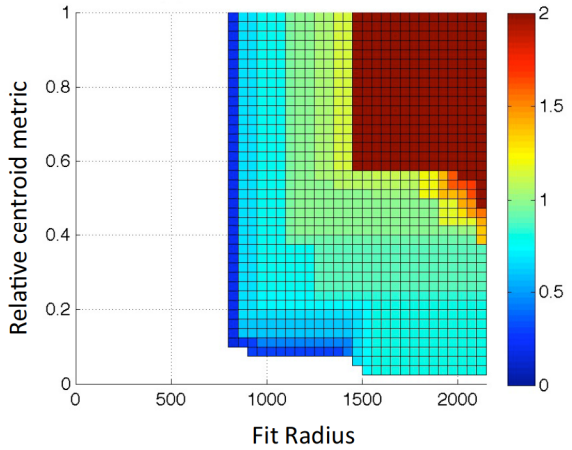

Figure 8. Current WAAS undersampled ionospheric threat model.

The Threat Due To Irregularities That Occur During Extreme Ionospheric Storms

It has been observed that the largest contributions to the ionospheric threat model typically arise during the recovery periods that follow the onset of highly disturbed ionospheric conditions associated with *extreme ionospheric storms*.[7] A dramatic example of such a storm occurred over Halloween in 2003. It began at approximately 16:00 UTC on 29 October 2003, when a coronal mass ejection collided with the earth, initiating a large disruption of the ionosphere that lasted more than forty-eight hours. The occurrence of such storms generally coincides with a strong drop in the geomagnetic D_{st} index. The observed total electron content is characterized by unusually large magnitudes and strong gradients over an extensive geographic region. The Halloween storm, for example, generated vertical delay values at mid-latitudes that

exceeded 200 TECU (where 1 TECU corresponds to 10^{16} electrons per meter^2). Storms of such magnitude occur only rarely over the course of a solar cycle (*e.g.*, 5 – 10 times per 11-year cycle).

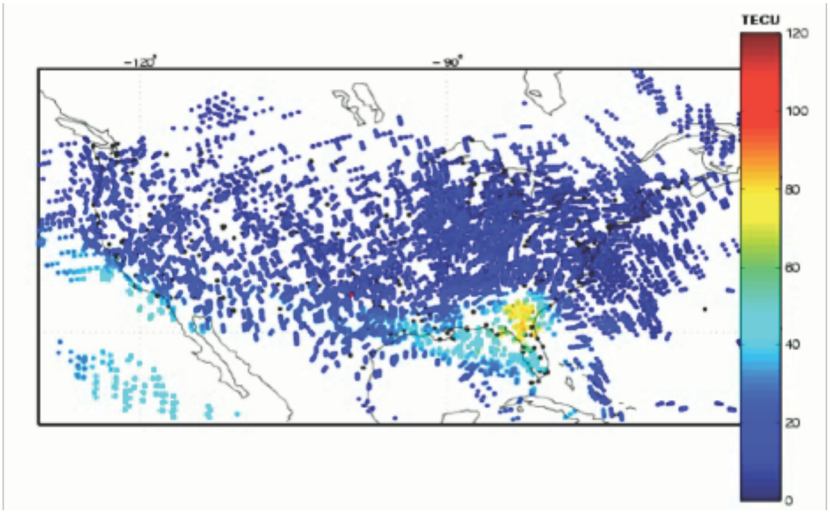

Figure 9. The vertical ionospheric delay (in TECU) over the southeastern United States, sampled by the CORS network between 3:45 and 4:00 UTC, 31 October 2003.

Under nominal conditions during the night, electrons in the ionosphere undergo extensive recombination with atmospheric ions, and the electron density generally diminishes to a very small magnitude. Following the second day of the Halloween storm, however, a dense, highly localized remnant of a daytime disturbance persisted for many hours into the early morning. This disturbance hovered over northern Florida for several hours and has subsequently become known as the *Florida event*. This event can be seen in Figure 9 which shows the vertical delay over the southeastern United States as sampled by a dense set of receivers in the CORS network between 3:45 and 4:00 UTC, 31 October 2003.

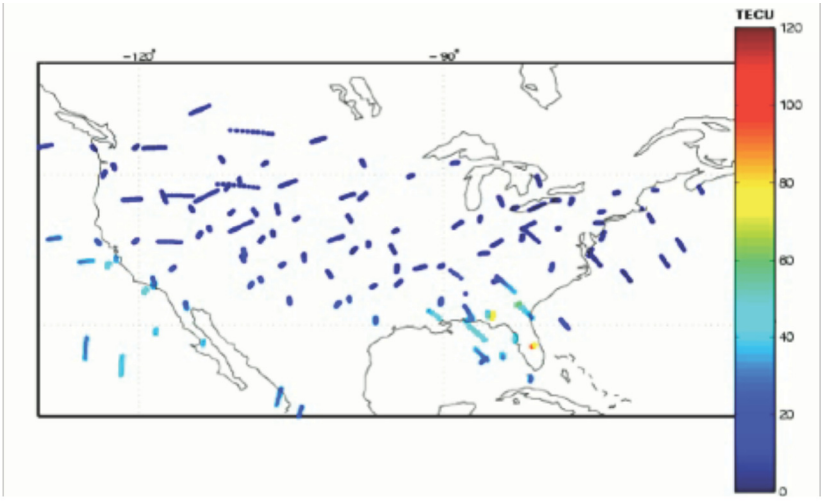

Figure 10. The vertical ionospheric delay (in TECU) over the southeastern United States, sampled by the WAAS network between 3:45 and 4:00 UTC, 31 October 2003.

Figure 10 shows the same event over the same duration as sampled by receivers in the WAAS network. Throughout the duration of this event, WAAS detected the irregularity and responded appropriately. No misleading information was broadcast. This was somewhat fortuitous, however. Given the highly localized nature of the irregularity, it is evident that it might possibly have gone undetected had it been oriented slightly differently.

The observation that the Florida event could potentially have caused large, undetectable errors in the delay estimates generated from WAAS IGDs was a source of considerable consternation in the WAAS program. It motivated the development of the *extreme storm detector*. The extreme storm detector in WAAS identifies the onset of an extreme storm and defines a period over which delay estimates at all grid points in the system are declared unusable. When this period extends well beyond the recovery period of the storm, users are protected from errors arising from the failure of local irregularity detectors to sample irregularities such as those depicted in Figure 9.

The extreme storm detector relies on a *regional disturbance metric* (*RDM*) to characterize the level of disturbance over the entire WAAS coverage area as a function of time. In the development of the extreme storm detector, many candidates were considered to serve as the *RDM* – the metric chosen was one of the simplest: in a given epoch the *RDM* is the maximum value that the irregularity metric assumes at any IGP (see Figure 6). The extreme storm detector trips when the *RDM* has risen above a storm onset threshold and has remained above it continuously over a specified onset confirmation interval. The nominal state of the extreme storm detector is restored after the *RDM* drops below a specified recovery threshold and remains below the onset threshold continuously over a specified hysteresis period, also known as the recovery confirmation interval. Figure 11 shows the time history of the RDM for two storms: (a) a moderate storm that occurred on 31 March 2001 and (b) the Halloween storm of 29-31 October 2003.

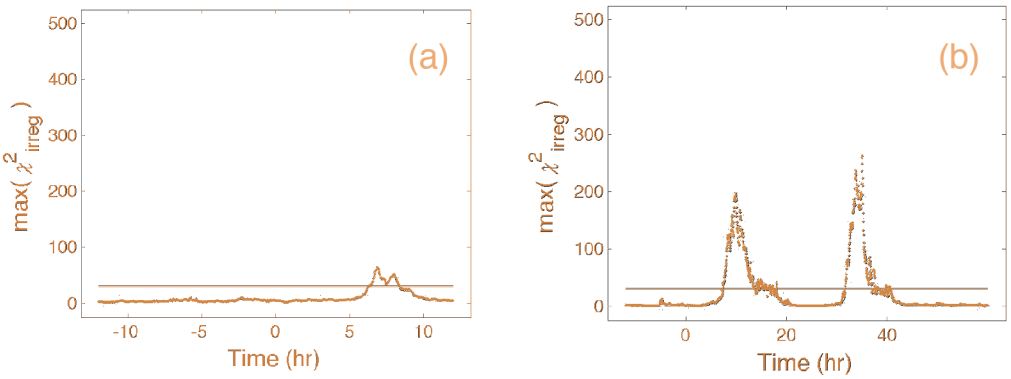

Figure 11. The regional disturbance metric as a function of time for (a) the moderate storm of 31 March 2001 and (b) the extreme storm of 29-31 October 2003. Also displayed in each figure are the onset and recovery thresholds of the extreme storm detector (spaced closely together).

In WAAS, the integrity burden for detecting the presence of ionospheric irregularities is shared between the local irregularity detector and the system-wide extreme storm detector. When generating the undersampled ionospheric threat model, no data are tabulated locally when an irregularity detector has tripped or globally when the extreme storm detector has tripped. In the absence of an extreme storm detector, disturbances such as the Florida event would require a dramatic increase in the augmentation of the GIVE provided by the threat model, thereby reducing WAAS availability under nominal ionospheric conditions.

RANKING IONOSPHERIC STORMS

Prior to each upgrade of WAAS that involves modifications of the algorithms used to generate the IGDs and GIVEs, it is necessary to conduct a thorough analysis of these algorithms to verify their safety and integrity for airline navigation. Included in this analysis is an assessment of the relationship between a storm and its impact on the ionospheric threat model. To perform this analysis, it has proven useful to devise a scalar metric to characterize the overall magnitude of the storm. Since the storm magnitude will tend to increase with the magnitude of the regional disturbance metric, an obvious candidate for the storm magnitude metric is the maximum instantaneous value of the *RDM* over the course of the storm. This choice, however, fails to take into account the temporal duration of the storm: a storm that attains a given maximum *RDM* can be expected to have a larger impact the longer it endures.

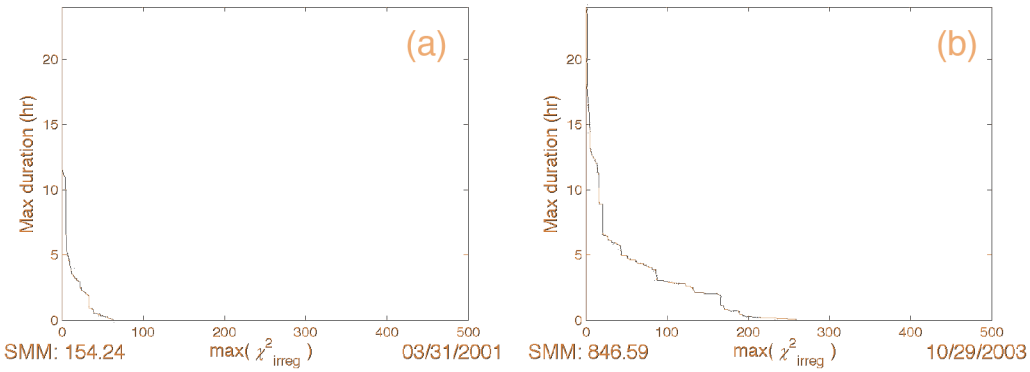

Figure 12. Storm profiles for the two storms displayed in Figure 11.

To take into account the duration of a storm, WAAS evaluates a scalar metric based upon the concept of a *storm profile*. A storm profile is defined to be the function $P(\chi^2)$ such that, for a given value χ^2, $P(\chi^2)$ is the maximum duration over which $RDM = \max[\chi^2_{irreg}]$ remains *continuously* above χ^2. The storm magnitude metric (*SMM*) is then defined to be the area under the curve. This metric takes into account both the maximum instantaneous level of disturbance and the temporal duration of the disturbance at a given level. Figure 12 shows the storm profiles corresponding to regional disturbance metrics displayed in Figure 11. The SMMs for these storms, *i.e.*, the areas under each curve, are 154.2 and 846.6, respectively.

Figure 13 shows how the largest storms of the last solar cycle rank according to the storm magnitude metric. This metric clearly differentiates known extreme storms, *i.e.*, the top four storms (with potentially hazardous electron density gradients) from the more moderate storms.

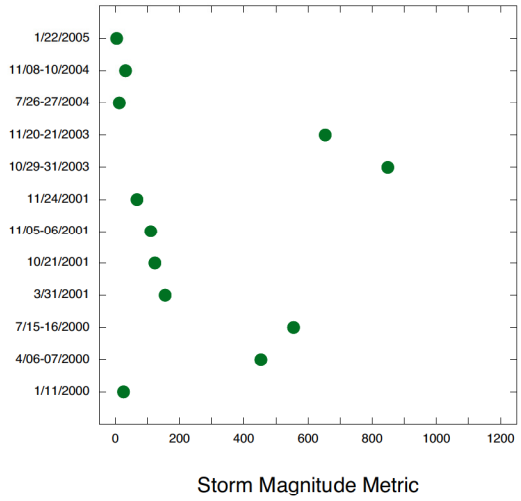

Figure 13. The storm magnitude metric for each of the major ionospheric storms of the last solar cycle.

SUMMARY

This paper has provided an overview of how a representative global navigation satellite system, the United States' Wide Area Augmentation System, protects airline navigation from positioning error due to space weather. The presence of ionospheric disturbances can cause significant error in the gridded vertical delay estimates that WAAS broadcasts. Consequently, WAAS must monitor the state of the ionosphere continuously.

The threats posed by ionospheric irregularities may be classified according to three distinct types: well-sampled irregularities, undersampled irregularities, and highly localized irregularities that occur during the recovery periods of extreme ionospheric storms. To monitor the state of the ionosphere, WAAS relies on an irregularity detector at each ionospheric grid point and on an extreme storm detector globally. When these detectors trip, vertical delay estimates broadcast by WAAS are declared to be unavailable for position calculations. By these means, WAAS guarantees that airline navigation based upon GPS signals will not be subject to dangerous positioning errors due to the occurrence of significant space weather events.

ACKNOWLEDGMENTS

Research in support of WAAS has been performed at the Jet Propulsion Laboratory/California Institute of Technology under contract to the National Aeronautics and Space Administration and the Federal Aviation Administration.

---

[1] Sparks, L., J. Blanch, and N. Pandya, "Estimating ionospheric delay using kriging: 1. Methodology." *Radio Sci.*,*46*, RS0D21, doi:10.1029/2011RS004667, 2011.

[2] Walter, T., A. Hansen, J. Blanch, P. Enge, A. Mannucci, X. Pi, L. Sparks, B. Iijima, B. El-Arini, R. Lejeune, M. Hagen, E. Altshuler, R. Fries, and A. Chu, "Robust Detection of Ionospheric Irregularities." *Navigation 48,* 89-100, 2000.

[3] Sparks, L., J. Blanch, and N. Pandya, "Estimating ionospheric delay using kriging: 2. Impact on satellite-based augmentation system availability." *Radio Sci.*,*46*, RS0D22, doi:10.1029/2011RS004781, 2011.

[4] Sparks, L. X. Pi, A. J. Mannucci, T. Walter, J. Blanch, A. Hansen P. Enge, E. Altshuler, and R. Fries, "The WAAS ionospheric threat model." *Proceedings of the International Beacon Satellite Symposium*, Boston College, Boston, MA, 2001.

[5] Altshuler, E. R. Fries, and L. Sparks, "The WAAS ionospheric threat model." *Proceedings of the 14th International Technical Meeting of the Satellite Division of the Institute of Navigation* (ION GPS 2001), Salt Lake City, UT, 2001.

[6] Paredes, E., N. Pandya, L. Sparks, and A. Komjathy, "Reconstructing the WAAS undersampled ionospheric gradient threat model for the WAAS expansion into Mexico." *Proceedings of the 21st International Technical Meeting of the Satellite Division of the Institute of Navigation* (ION GSS 2008), Savannah, Ga, 2001.

[7] Sparks, L. A. Komjathy A.J. Mannucci, E. Altshuler, T. Walter, J. Blanch, M. Bakry El-Arini, and R. Lejeune, "Extreme ionospheric storms and their impact on WAAS." *Proceedings of the 2005 Ionospheric Effects Symposium*, Alexandria, VA, 2005.